Average Age-of-Information Minimization in EH-enabled Low-Latency IoT Networks

Yao Zhu[†,‡], Xiaopeng Yuan[†,‡], Bin Han[§], Yulin Hu[†,‡] and Anke Schmeink[‡]
[†]School of Electronic Information, Wuhan University, China, Email: $yulin.hu$@ieee.org
[‡]ISEK Research Area, RWTH Aachen, Germany, Email: $zhu|yuan|schmeink$@isek.rwth-aachen.de
[§]Technische Universität Kaiserslautern, Germany, Email: $binhan$@eit.uni-kl.de

***Abstract*—In this work, we study an energy harvesting (EH)-enabled low-latency communication network where a full-duplex server continuously performs wireless power transfer (WPT) to a half-duplex sensor. The sensor is designed to operate periodically in each updating round, during which the sensor firstly harvests energy via the WPT process, then collects measurement data and wirelessly transmits an update to the server based on the harvested energy. We assume that no energy can be reserved at the end of each round, due to the deployed capacitor-structured energy container. Leveraging the recent characterization on the error probability in the finite blocklength (FBL) regime, we derive the average Age-of-Information (AoI) in the considered network and construct a problem minimizing the average AoI via optimizing the duration of the updating round. The convexity of the optimization problem is shown, following which an efficient optimal solution is provided. At last, via Monte Carlo simulations, the convexity of the problem can also be visualised, and the average AoI performance of the network is evaluated.**

***Index Terms*—Energy harvesting (EH), internet of things (IoT), age of information (AoI), finite block length (FBL).**

I. Introduction

In wireless sensor networks (WSNs), the limited battery storage at sensors has become a key restriction in network operation [1]. The required manual battery exchange and possible energy refilling have resulted in high expenses, especially when massive devices are involved in a network [2]. To get rid of the energy constraint in wireless networks, radio-frequency (RF) energy harvesting (EH) technologies have been deployed and proved to be capable of prolonging the battery lifetime of devices [3], [4]. In particular, by merging the EH technologies into wireless networks, the wireless powered communication networks (WPCNs) have been enabled with all devices being powered by wireless energy transmitters [5]–[7]. Due to the high controllability and high flexibility on power transfer, WPCNs have attracted abundant researchers and been investigated in multifarious applications. In [8]–[10], the authors have assumed the network performs wireless power transfer (WPT) and information transmission separately, where WPT is applied in the downlink for harvesting energy to the devices, then the information is transmitted via uplink channels with the harvested energy. By optimizing the allocations of time resource and power resource, both the network throughput [8], [9] and the energy efficiency [10] have been improved in WPCNs. Moreover, by exploiting the strategy of simultaneously wireless information and power transfer (SWIPT) [3], WPCNs have also been extended into relaying networks, where both the energy and information are loaded on the signal from a source node and the carried energy is harvested by a relay node. Then, the relay forwards the information with obtained energy. In existing literature, the related relaying schemes have been explored for improving the network capacity [11], reducing the transmit power under reliability constraints [12] and maximizing the network utility [13].

On the other hand, the freshness of information also plays a critical role in real-time operations [14]. As a novelty metric of transmitted data message, the concept of age of information (AoI) has been introduced in [14] to indicate such freshness [15]. So far, AoI has been extensively characterized in copious wireless networks, such as multi-hop networks [16], broadcasting networks [17], edge computing networks [18], and networked control loops [19]. In particular, AoI is also analyzed in WPCNs. Since a lower value of AoI generally stands for an advanced data freshness, the AoI has been minimized for WPCN in literature via designing the updating policies with a relay node in [20] and with cognitive radio in [21].

However, all existing works [20]–[23] regarding AoI in WPCNs have assumed error-free channels. Clearly, with infinite blocklength (IBL), a coding rate lower than the Shannon capacity is sufficient for an error-free data transmission. By contrast, confirmed in [24], with a finite blocklength (FBL), data transmission may still result in an error probability regardless of blocklength, which is not negligible. To the best of our knowledge, although AoI has been studied in the FBL regime in [25], while considering the impact of finite blocklength, a characterization of AoI in WPCNs has not been performed yet. This motivated us to exploit the characterization of the decoding error probability with FBL codes [24] and focus on the average AoI in WPCN.

In this paper, we consider a simple IoT network with one full-duplex server and one half-duplex sensor. The sensor is wirelessly powered by the server, collects and transmits information update based on the accumulated harvested energy. We

Y. Hu is the corresponding author.

Fig. 1. An example of considered system

first characterize the average AoI while the network performs periodic updating rounds. Then, we focus on the average AoI minimization problem with the round duration to be optimized. Under constraints of error probability and SINR, we rigorously prove the convexity of the interested optimization problem, with which the problem can be efficiently optimally addressed. Finally, via Monte Carlo simulations, the convexity of the focused problem is validated, and the impacts of FBL codes and coding rate are observed.

The remaining part of the paper is organized as follows. In Section II, we introduce the system model. Section III characterizes the AoI performance under the consideration of the FBL impact. In section IV, the optimization problem is formulated and the analytical solution is provided. The Monte Carlo simulation results are presented in Section V, and finally, the conclusions are drawn in Section VI.

II. System Model

Consider an IoT network, where a server requires local information update with data size of d bits (for each update) from a sensor continuously. We assume the sensor to be an active source, i.e., the most recent information is available upon request. The sensor is passive and mounted with capacitors to store energy. Note that the sensor is assumed to have no rechargeable battery and the operation fully relies on the wireless power transfer (WPT) via radio frequency from the server. The server enables a full-duplex model, where the wireless information transfer (WIT) is carried out in the same channel of WPT. With a continuously existing signal from the source for energy harvesting, no downlink communication is enabled in the occupied channel, i.e., the sensor receives no acknowledgement from the server. Since the information update is carried out circularly, we consider that all behaviors of the sensor between the previous update and the current update belong to an information updating round. In particular, each round can be broken down into three phases: i) the sensor harvests radio energy from the server over charging time t_c, while receiving energy E_c; ii) Then, it collects the current information with collecting time t_s, while spending energy E_s; iii) Finally, it transmits the data via a wireless channel over transmission time t_r, while consuming energy E_r. Due to the simple circuit with a single antenna in the sensor, the operation of each phase is mutually exclusive from another, i.e., the sensor cannot harvest energy while transmitting data. Therefore, the sensor is operated in a half-duplex mode. Denoting by T_S the duration of one symbol, the blocklength of transmission $n = \frac{t_r}{T_S}$ belongs to the finite blocklength regime, namely, $20 \leqslant n \leqslant 2000$. As a result, the total time duration for a single information updating round T is given by

$$T = t_c + t_s + t_r. \tag{1}$$

On the other hand, the total energy consumption cannot exceed the total harvested energy gain, i.e., $E_c \geqslant E_r + E_s$. Furthermore, since there is no dedicated battery on the sensor, we assume the surplus of unspent energy from the current round cannot be reserved to the next one and the transmission should be carried out with short blocklength/short packet to avoid a power leakage from the capacitor. Note that the energy conversion is not perfect. In this work, we consider an energy harvest efficiency $\mu \leqslant 1$. Let z denote the channel gain between the sensor and the server. Then, the harvested energy over charging time t_c is given by

$$E_c = \mu \frac{z P_c}{\zeta} t_c, \tag{2}$$

where P_c is the transmit power of the server and ζ is the pass loss. After collecting the data, sensor transmits the packet using the harvested energy. Therefore, the transmit power of sensor P_r depends on the amount of energy left and the duration of transmission, i.e.,

$$P_r = \frac{E_r}{t_r} \leqslant \frac{E_c - E_s}{t_r}. \tag{3}$$

At the server side, via self-interference cancellation technologies, transmission and reception are enabled to be operated simultaneously. Due to the imperfect cancellation, the residual interference is not negligible. We denote by h the power gain of the residual loop interference. As a result, the signal-to-interference-noise ratio (SINR) at the server side γ_r is given by

$$\gamma_r = \frac{z P_r}{\zeta} \frac{1}{\sigma^2 + h P_c}, \tag{4}$$

where σ^2 is the noise power and we assume the channel to be constant within the three phases and perfectly known, due to the short collecting and transmission time.

III. Characterization of Coding Error Probability and Age-of-Information

A. Decoding Error Probability with Short Packet

The updating round is considered as a failure(success), if the error (not) occurs during decoding the transmitted information update. Recall that short packets are exploited for the transmission of the information update. The decoding error probability is significantly influenced by SINR γ_r, even when the coding rate is lower than the Shannon capacity. In particular, with a blocklength $n = \frac{t_r}{T_S}$ and a coding rate r, the

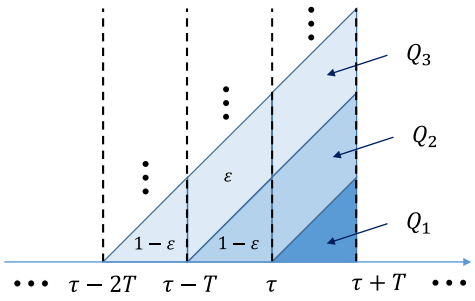

Fig. 2. Illustration of AoI. The transparency indicates the likelihood of the area that contributes in AoI.

decoding error probability of any information update at the server side is given by [24]

$$\varepsilon = \mathcal{P}(\gamma_r, r, n) \approx Q\Big(\sqrt{\tfrac{n}{V(\gamma_r)}}(\mathcal{C}(\gamma_r) - r)\log_e 2\Big), \quad (5)$$

where $r = \frac{dT_S}{t_r}$ is the coding rate (in bit/symbol) and $\mathcal{C} = \log_2(1+\gamma_r)$ is the Shannon capacity. In addition, $V = \frac{2\gamma+\gamma^2}{(1+\gamma)^2}$ is the channel dispersion. Note that sensor receives neither Acknowledge (ACK) nor Negative Acknowledgement (NACK) from server. Furthermore, the sensor always transmits the most recent information and discards the previous one regardless of a success or a failure. Therefore, the error probability of each transmission is independent and identically distributed. Considering an arbitrary current round, denote by X_k the event that the transmission succeeds at previous k^{th} round, while all rounds between the previous k^{th} round and the current round fail. Then, the probability of the event X_k is given by

$$\mathsf{P}(X_k) = \left(1 - \varepsilon(\gamma_r, r, \frac{t_r}{T_s})\right)\varepsilon^{k-1}(\gamma_r, r, \frac{t_r}{T_s}), \forall k \geqslant 1. \quad (6)$$

B. Time-Average Age-of-Information

The instantaneous AoI $\Delta(\tau)$ at time instance τ is defined by the freshness of information, i.e.,

$$\Delta(\tau) = \tau - U(\tau), \quad (7)$$

where $U(\tau)$ is the time instance of the most recently received information update on the server. Clearly, $\Delta(\tau)$ is a linear increasing function w.r.t. τ within the interval of any round, i.e., $\tau \in [\tau_0, \tau_0+T)$. Note that the update is only considered as received, if the transmitted data packet is successfully decoded by the server. Therefore, for any current round at any time, the AoI depends on how many failure rounds are there between the current round 0 and the last previous successful round k, where $k > 0$. In particular, if X_k is true, the accumulative AoI over the interval is represented by the sum of all parallelogram areas Q_k and triangle area Q_1, which are illustrated in Fig. 2. Therefore, Q_k is given by

$$Q_k = \begin{cases} \frac{1}{2}T^2, & k = 1, \\ T^2, & \text{Otherwise.} \end{cases} \quad (8)$$

Then, the time-average AoI can be written as

$$\begin{aligned} \mathbb{E}[\Delta] &= \lim_{\tau_0\to\infty} \frac{\sum_{k=1}^{K} \mathsf{P}(X_k)(\sum_{i=1}^{k} Q_i)}{\tau_0 + T - \tau_0} \\ &= \lim_{\tau_0\to\infty} \sum_{k=1}^{K} \left(k - \frac{1}{2}\right) T\left(\varepsilon^{k-1} - \varepsilon^k\right) \\ &= \lim_{\tau_0\to\infty} \left(\frac{1}{2}T + \sum_{k=1}^{K-1} k\varepsilon^k T - \varepsilon^K\left(K - \frac{1}{2}\right)T\right) \\ &= \frac{1}{2}T + \sum_{k=1}^{\infty} k\varepsilon^k T, \end{aligned} \quad (9)$$

where $K = \frac{\tau_0}{T}$ is the number of information updating rounds, which approaches to infinity when $\tau_0 \to \infty$, and $\varepsilon = \varepsilon(\gamma_r, r, \frac{t_r}{T_s})$. Since $K \to \infty$ as $\tau_0 \to \infty$, the term of polynomial series sum vanishes for all $\varepsilon \leqslant \varepsilon_{\max}$, where $\varepsilon_{\max} \leqslant 0.1$ is the error probability threshold.

IV. Time-Average AoI Minimization

Based on the above characterizations, we aim at minimizing the time-average AoI $\mathbb{E}[\Delta]$ by optimizing the time duration of each round T, while fulfilling error probability and SINR constraints. The optimization problem is formulated as

$$\begin{aligned} \underset{T}{\text{minimize}} \quad & \mathbb{E}[\Delta] && (10a) \\ \text{subject to} \quad & \varepsilon \leqslant \varepsilon_{\max}, && (10b) \\ & \gamma_r \geqslant \gamma_{\min}, && (10c) \\ & E_r + E_s \leqslant E_c, && (10d) \\ & T = t_c + t_s + t_r, && (10e) \end{aligned}$$

where constraint (10b) and (10c) ensure the quality of transmission to prevent a waste of energy, where $\varepsilon_{\max} \leqslant 0.1$ is the error probability threshold and $\gamma_{\min} \geqslant 0$dB is the SINR threshold. Since the coding rate r and the collect time t_s are fixed, for any given information bits d, the transmission duration $t_r = \frac{d}{r}$ is also fixed for each transmission. Therefore, the variable T appears as a linear function of t_c, and to optimize T is essentially equivalent to choose how long the sensor should be charged, i.e., selecting t_c. Moreover, it is trivial to show that the equality of constraint (10d) should hold for the optimal solution, as it is always beneficial to spend all charged energy instead of discarding any amount of it. Therefore, by taking (9) into account, the optimization problem (10) can be reformulated as

$$\begin{aligned} \underset{t_c}{\text{minimize}} \quad & \frac{1}{2}T + \sum_{k=1}^{\infty} k\varepsilon^k T && (11a) \\ \text{subject to} \quad & \varepsilon \leqslant \varepsilon_{\max}, && (11b) \\ & \gamma_r \geqslant \gamma_{\min}, && (11c) \\ & E_r + E_s = E_c. && (11d) \end{aligned}$$

Then, we have the following key lemma to characterize the reformulated problem:

Lemma 1. *All the constraints in problem* (11) *are convex. And under the constraints, the objective function of problem* (11) *is also convex in* t_c.

Proof. First, we show the convexity of the error probability. Based on (2), (4) and constraint (11d), we have

$$\begin{aligned}\gamma_r &= \frac{z}{\zeta}\frac{1}{\sigma^2+hP_c}\frac{E_c-E_s}{t_r} \\ &= \frac{\mu z^2 P_c}{\zeta^2 t_r(\sigma^2+hP_c)}t_c - \frac{zE_s}{\zeta(\sigma^2+hP_c)t_r}.\end{aligned} \tag{12}$$

Then, the first-order derivative w.r.t. t_c using the chain rule is given by

$$\frac{\partial \varepsilon}{\partial t_c} = \frac{\partial \varepsilon}{\partial \omega}\frac{\partial \omega}{\partial \gamma_r}\frac{\partial \gamma_r}{\partial t_c}, \tag{13}$$

where $\omega = \sqrt{\frac{n}{V}}(\mathcal{C}(\gamma_r) - r)$.

Similarly, the second-order derivative is given by

$$\begin{aligned}\frac{\partial^2 \varepsilon}{\partial t_c^2} =& \frac{\partial^2 \varepsilon}{\partial \omega^2}\left(\frac{\partial \omega}{\partial \gamma_r}\frac{\partial \gamma_r}{\partial t_c}\right)^2 + \frac{\partial \varepsilon}{\partial \omega}\frac{\partial^2 \omega}{\partial \gamma_r^2}\left(\frac{\partial \gamma_r}{\partial t_c}\right)^2 \\ &+ \frac{\partial \varepsilon}{\partial \omega}\frac{\partial \omega}{\partial \gamma_r}\frac{\partial^2 \gamma_r}{\partial t_c^2}.\end{aligned} \tag{14}$$

For each component of the derivative, which is also in the form of the derivative, we have

$$\frac{\partial \varepsilon}{\partial \omega} = -\frac{1}{\sqrt{2\pi}}e^{-\frac{\omega^2}{2}}, \tag{15}$$

$$\frac{\partial^2 \varepsilon}{\partial \omega^2} = \frac{1}{\sqrt{2\pi}}\omega e^{-\frac{\omega^2}{2}}, \tag{16}$$

$$\frac{\partial \omega}{\partial \gamma_r} = \frac{\sqrt{n}(r+\gamma_r(\gamma_r+2)-\log(\gamma_r+1))}{(\gamma_r(\gamma_r+2))^{\frac{3}{2}}}, \tag{17}$$

$$\begin{aligned}\frac{\partial^2 \omega}{\partial \gamma_r^2} =& \frac{\sqrt{n}}{\sqrt{(\gamma_r+1)^2\gamma_r^5(\gamma_r+2)^5}}\cdot \\ &\left(-3r(\gamma_r+1)^2 - \gamma_r(\gamma_r+2)(\gamma_r^2+2\gamma_r+2)\right. \\ &\left.+3(\gamma_r+1)^2\log(\gamma_r+1)\right),\end{aligned} \tag{18}$$

$$\frac{\partial \gamma_r}{\partial t_c} = \frac{\mu z^2 P_c}{\zeta^2 t_r(\sigma^2+hP_c)}, \tag{19}$$

and

$$\frac{\partial^2 \gamma_r}{\partial t_c^2} = 0. \tag{20}$$

By merging (15)-(20) into (14), it can be rewritten as

$$\frac{\partial^2 \varepsilon}{\partial t_c^2} = \frac{1}{\sqrt{2\pi}}e^{-\frac{\omega^2}{2}}\left(\omega\left(\frac{\partial \omega}{\partial \gamma_r}\right)^2 - \frac{\partial^2 \omega}{\partial \gamma_r^2}\right)\left(\frac{\partial \gamma_r}{\partial t_c}\right)^2. \tag{21}$$

With the condition that the coding rate does not exceed the Shannon capacity, i.e., $\mathcal{C}(\gamma_r) \geqslant r$, it holds $\omega \geqslant 0$. Furthermore, from [4], we have $\frac{\partial^2 \omega}{\partial \gamma_r^2} \leqslant 0$, if $\gamma_r \geqslant 1$. As a result, it holds that $\frac{\partial^2 \varepsilon}{\partial t_c^2} \geqslant 0$, i.e., constraint (11b) is convex.

It is trivial to show that the constraint (11c) is convex and constraints (11d) is affine. Therefore, all the constraints of (11) are either convex or even affine.

Next, we move on to the convexity of the objective function $\mathbb{E}[\Delta]$ w.r.t. t_c. We define $f_k = k\varepsilon^k T$. For any $k \geqslant 1$, we have

$$\frac{\partial^2 f_k}{\partial t_c^2} = k(k-1)\varepsilon^{k-2}t_c(\varepsilon')^2 + k\varepsilon^{k-1}\left(\frac{\partial^2 \varepsilon}{\partial t_c^2}t_c + 2\frac{\partial \varepsilon}{\partial t_c}\right). \tag{22}$$

Since all other terms in (22) are non-negative, we focus on the sign of $\frac{\partial^2 \varepsilon}{\partial t_c^2}t_c + 2\frac{\partial \varepsilon}{\partial t_c}$. With the condition $\varepsilon \leqslant \varepsilon_{\max} \leqslant 0.1$, i.e., $\omega \geqslant Q^{-1}(0.1) \geqslant 1.25$, and based on (12), we have (23)

$$\begin{aligned}&\frac{\partial^2 \varepsilon}{\partial t_c^2}t_c + 2\frac{\partial \varepsilon}{\partial t_c} \\ =& A_1\left(\omega\left(\frac{\partial \omega}{\partial \gamma_r}\right)^2(\gamma_r+A_2) - \frac{\partial^2 \omega}{\partial \gamma_r^2}(\gamma_r+A_2) - 2\frac{\partial \omega}{\partial \gamma_r}\right) \\ \geqslant& A_1\left(\underbrace{\left(1.25\frac{\partial \omega}{\partial \gamma_r}\gamma_r - 2\right)}_{B}\frac{\partial \omega}{\partial \gamma_r} - \frac{\partial^2 \omega}{\partial \gamma_r^2}\gamma_r\right) \\ &+ A_1A_2\left(\omega\left(\frac{\partial \omega}{\partial \gamma_r}\right)^2 - \frac{\partial^2 \omega}{\partial \gamma_r^2}\right),\end{aligned} \tag{23}$$

where the constants $A_1 = \frac{1}{\sqrt{2\pi}}e^{-\frac{\omega^2}{2}}\frac{\mu z^2 P_c}{\zeta^2 t_r(\sigma^2+hP_c)} \geqslant 0$ and $A_2 = \frac{zE_s}{\zeta(\sigma^2+hP_c)t_r} \geqslant 0$. Furthermore, for any $n \geqslant 20$ and $\gamma_r \geqslant 1$, we have that

$$\begin{aligned}B =& \frac{1}{\sqrt{\gamma_r(\gamma_r+2)^3}}\cdot\left(1.25\sqrt{n}(\gamma_r^2+2\gamma_r+r)\right. \\ &\left.-1.25\sqrt{n}\log(\gamma_r+1) - 2\sqrt{\gamma_r(\gamma_r+2)^3}\right) \geqslant 0.\end{aligned} \tag{24}$$

In the meantime, we can also show that

$$\begin{aligned}\frac{\partial \omega}{\partial \gamma_r} &= \frac{\sqrt{n}(r+\gamma_r(\gamma_r+2)-\log(\gamma_r+1))}{(\gamma_r(\gamma_r+2))^{\frac{3}{2}}} \\ &= \frac{\sqrt{n}(r+\gamma_r(\gamma_r+1)+\gamma_r-\log(\gamma_r+1))}{(\gamma_r(\gamma_r+2))^{\frac{3}{2}}} \\ &\geqslant \sqrt{n}\frac{r+\gamma_r(\gamma_r+1)}{(\gamma_r(\gamma_r+2))^{\frac{3}{2}}} \geqslant 0,\ \forall \gamma_r \geqslant 1.\end{aligned} \tag{25}$$

As a result, it holds that $\frac{\partial^2 f_k}{\partial t_c^2} \geqslant 0$ for any $k \geqslant 1$, i.e., f_k is convex in t_c. As the sum of convex function, the objective function $\frac{1}{2}T + \sum_{k=1}^{\infty} k\varepsilon^k T$ is also convex in t_c. □

We have shown in Lemma 1 that the objective function is convex and all constraints in Problem (11) are either convex or affine. Hence, Problem (11) is a convex one, i.e., Problem (11) can be solved optimally and efficiently via standard convex programming method tools.

V. Simulation Results

In this section, via Monte Carlo simulations we validate our analytical results and evaluate the system performance. In all simulations, we consider the following parameterization. First, we set the transmit power of server to $P_s = 30$ dBm. In addition, the distance between server and sensor is 5 m and

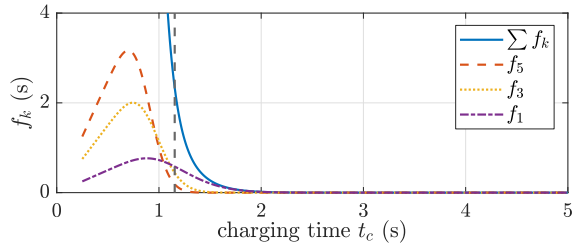

(a) values of individual f_k and sum of f_k versus charging time t_c. The horizontal line indicates the convex regime.

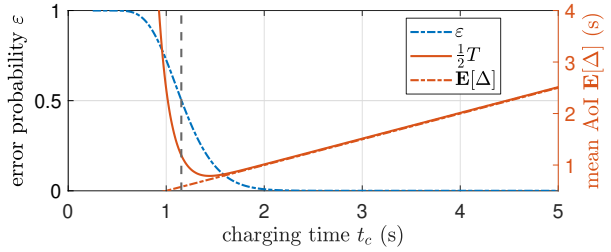

(b) error probability ε and average AoI $\mathbb{E}[\Delta]$ versus charging time t_c. The horizontal line indicates the convex regime.

Fig. 3. The impact of charging time t_c on component f_k Average AoI $\mathbb{E}[\Delta]$ and error probability ε. The dashed lines indicate the charging time, where $\varepsilon = \varepsilon_{\max}$.

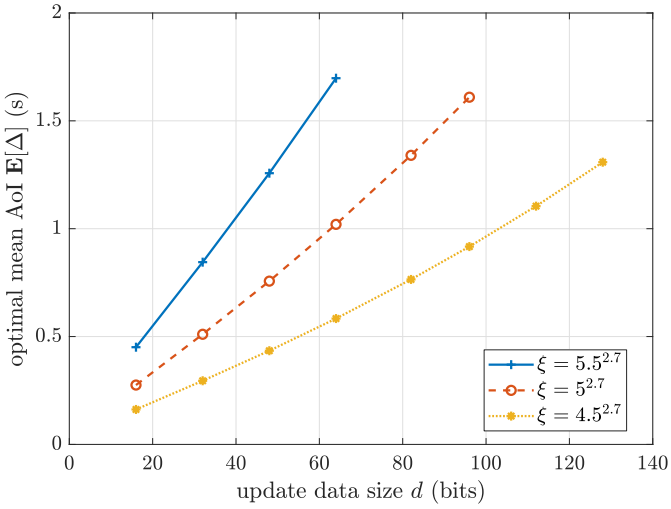

Fig. 4. Optimal mean AoI $\mathbb{E}[\Delta]^*$ versus information bits d while varying the distance between server and sensor for 4.5 m, 5 m and 5.5 m.

consider a path-loss exponent of 2.7, i.e., path loss $\xi = 5^{2.7}$, and the gain of channel fading is set to $z = 1$. Moreover, The noise power level is -20 dBm. The information amount of update is $d = 50$ bits and considered as constant for each update, which is transmitted over $t_r = 3.2$ ms with duration of symbol $T_s = 0.025$ ms. Finally, the simulation is carried out with total running time $\max \tau = 3600$ s.

We start with Fig. 3 to present the impact of charging time t_c on the system. In particular, we plot a) average AoI $\mathbb{E}[\Delta]$ (as left y-axis) and decoding error probability ε (as right y-axis), as well as b) AoI component $f_k = k\varepsilon^k T$ versus charging time t_c. Note that the dashed vertical lines indicates the charging time, where it fulfills $\varepsilon = \varepsilon_{\max}$. we can see that both ε and $\mathbb{E}[\Delta]$ are convex in t_c when $\varepsilon \geqslant \varepsilon_{\max}$. In addition, a similar convexity can be also observed for f_k regardless the value of k. These observations confirm our analytical results in Lemma 1. Moreover, since f_k contains exponential error function with the order of k, the influence of high-order f_k on the average AoI is more significant with a lower t_c. When t_c is getting significantly longer, f_k vanishes due to the exponentially deceasing ratio and is eventually dominated by $\frac{1}{2}T$.

Next, we plot in Fig. 4 the optimal time-average AoI , i.e., the optimal value $\mathbb{E}[\Delta]^*$ of Problem (11), versus the number of information bits d. Different distances of the wireless links between the server and the sensor are considered. Since the error probability is monotonic function in d, $\mathbb{E}[\Delta]^*$ increases while d increasing regardless of different setups. However, the influence of information size on the optimal mean AoI becomes more significant when the distance between server and sensor is getting large. Meanwhile, when d is small, the gap of $\mathbb{E}[\Delta]^*$ tends to be closer. These observations match well with our analytical model. In fact, according to (9), when d approaches to 0, as all the terms related to f_k also vanish, $\mathbb{E}[\Delta]^* = 1/2T$ holds. On the other hand, when d goes too large so that the constraint $\varepsilon \leqslant \varepsilon_{\max}$ cannot be fulfilled (for any feasible values of t_c), the problem becomes infeasible. Note that a long distance has a negative influence on the SINR. Therefore, the feasible set of d is much shorter for the distance of 4.5 m, comparing to the one of 5.5 m.

To depict the impact of FBL codes, we study the optimal mean AoI $\mathbb{E}[\Delta]^*$ versus the blocklength for the information transmission n in Fig. 5. To compare with the impact of information bits, we choose the same setups of distance between server and sensor as 4.5 m, 5 m and 5.5 m, respectively. As expected, $\mathbb{E}[\Delta]^*$ decreases in n, and the decrease is in an exponential manner.Recall that we assume $t_c \gg t_r$. Therefore, even increasing n also implies a longer t_r, namely, a longer T, the influence on the average AoI is still negligible. Recall that the optimal $\mathbb{E}[\Delta]^*$ will also eventually converge to $\frac{1}{2}T$ when we keep increasing n. If the assumption of $t_c \gg t_r$ does not hold, it implies that the blocklength is infinite or sufficient long. Then, we can calculate the optimal solution for the infinite blocklength (IBL) regime. In particular, $\mathbb{E}[\Delta_{\text{IBL}}]^*$ is $\frac{1}{2}T$, when the inequality $\mathcal{C}(\gamma_r) \geq r$ is fulfilled. Moreover, similar to Fig. 5, we can also observe the different feasible intervals of n regarding to the distance between the user and the server. Combing the observation of both Fig. 4 and Fig. 5, adjusting the coding rate according the quality of channel is suggested, which makes the sensor to be able to transmit the update with a reasonable charging time.

VI. Conclusion

In this work, we have studied an EH-enabled IoT network, where a server operates in a full-duplex mode and transmits harvesting signals to a sensor and simultaneously receives

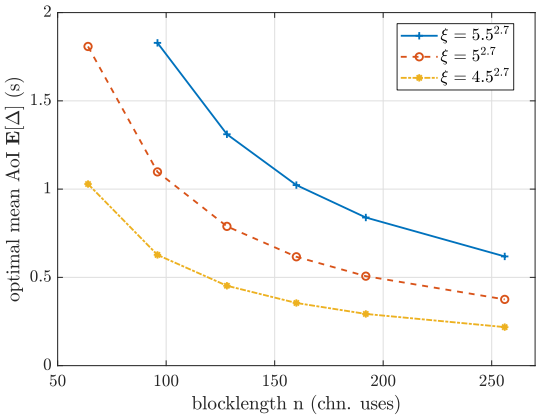

Fig. 5. Optimal mean AoI $\mathbb{E}[\Delta]^*$ versus blocklength n while varying the distance between server and sensor for 4.5 m, 5 m and 5.5 m.

the measurement update from the sensor. Within each single time duration length, the sensor is assumed to repeat a behaviour cycle of harvesting energy, collecting data and transmitting updates back to the server. The average AoI of the updates has been characterized, based on which we formulated an optimization problem minimizing the average AoI via determining the time length of the updating round. The problem is proved to be convex, i.e., the optimal solution can be efficiently obtained via convex optimization tools. Via simulations, we validate our analytical results and show the impact of information bits and blocklength on the AoI performance.

VII. Acknowledgement

The work in this paper has been supported by the German Research Council (DFG) within the basic research project DFG SCHM 2643/16. We gratefully acknowledge this support.

References

[1] V. Raghunathan, S. Ganeriwal and M. Srivastava, "Emerging techniques for long lived wireless sensor networks," *IEEE Communications Magazine*, vol. 44, no. 4, pp. 108-114, April 2006.

[2] S. Bi, C. K. Ho and R. Zhang, "Wireless powered communication: opportunities and challenges," *IEEE Communications Magazine*, vol. 53, no. 4, pp. 117-125, April 2015.

[3] X. Lu, P. Wang, D. Niyato, D. I. Kim and Z. Han, "Wireless Networks With RF Energy Harvesting: A Contemporary Survey," *IEEE Communications Surveys & Tutorials*, vol. 17, no. 2, pp. 757-789, Secondquarter 2015.

[4] Y. Hu, X. Yuan, T. Yang, B. Clerckx and A. Schmeink, "On the Convex Properties of Wireless Power Transfer With Nonlinear Energy Harvesting," *IEEE Transactions on Vehicular Technology*, vol. 69, no. 5, pp. 5672-5676, May 2020.

[5] S. Bi, Y. Zeng and R. Zhang, "Wireless powered communication networks: an overview," *IEEE Wireless Communications*, vol. 23, no. 2, pp. 10-18, April 2016.

[6] X. Lu, P. Wang, D. Niyato, D. I. Kim and Z. Han, "Wireless Networks With RF Energy Harvesting: A Contemporary Survey," *IEEE Communications Surveys & Tutorials*, vol. 17, no. 2, pp. 757-789, Secondquarter 2015.

[7] Y. Hu, Y. Zhu, M. C. Gursoy and A. Schmeink, "SWIPT-Enabled Relaying in IoT Networks Operating With Finite Blocklength Codes," *IEEE Journal on Selected Areas in Communications*, vol. 37, no. 1, pp. 74-88, Jan. 2019.

[8] L. Xie, J. Xu and R. Zhang, "Throughput Maximization for UAV-Enabled Wireless Powered Communication Networks," *IEEE Internet of Things Journal*, vol. 6, no. 2, pp. 1690-1703, April 2019.

[9] L. Xie, J. Xu and Y. Zeng, "Common Throughput Maximization for UAV-Enabled Interference Channel With Wireless Powered Communications," *IEEE Transactions on Communications*, vol. 68, no. 5, pp. 3197-3212, May 2020.

[10] Q. Wu, M. Tao, D. W. Kwan Ng, W. Chen and R. Schober, "Energy-Efficient Resource Allocation for Wireless Powered Communication Networks," *IEEE Transactions on Wireless Communications*, vol. 15, no. 3, pp. 2312-2327, March 2016.

[11] A. A. Nasir, X. Zhou, S. Durrani and R. A. Kennedy, "Relaying Protocols for Wireless Energy Harvesting and Information Processing," *IEEE Transactions on Wireless Communications*, vol. 12, no. 7, pp. 3622-3636, July 2013.

[12] I. Krikidis, "Simultaneous Information and Energy Transfer in Large-Scale Networks with/without Relaying," *IEEE Transactions on Communications*, vol. 62, no. 3, pp. 900-912, March 2014.

[13] H. Chen, Y. Li, Y. Jiang, Y. Ma and B. Vucetic, "Distributed power splitting for SWIPT in relay interference channels using game theory," *IEEE Transactions on Wireless Communications*, vol. 14, no. 1, pp. 410-420, Jan. 2015.

[14] S. Kaul, R. Yates and M. Gruteser, "Real-time status: How often should one update?," *2012 Proceedings IEEE INFOCOM*, Orlando, FL, 2012, pp. 2731-2735.

[15] M. A. Abd-Elmagid, N. Pappas and H. S. Dhillon, "On the Role of Age of Information in the Internet of Things," *IEEE Communications Magazine*, vol. 57, no. 12, pp. 72-77, December 2019.

[16] O. Ayan, H. Murat Gürsu, A. Papa and W. Kellerer, "Probability Analysis of Age of Information in Multi-Hop Networks," *IEEE Networking Letters*, vol. 2, no. 2, pp. 76-80, June 2020.

[17] J. Sun, Z. Jiang, S. Zhou and Z. Niu, "Optimizing Information Freshness in Broadcast Network with Unreliable Links and Random Arrivals: An Approximate Index Policy," *IEEE INFOCOM 2019 - IEEE Conference on Computer Communications Workshops (INFOCOM WKSHPS)*, Paris, France, 2019, pp. 115-120.

[18] X. Song, X. Qin, Y. Tao, B. Liu and P. Zhang, "Age Based Task Scheduling and Computation Offloading in Mobile-Edge Computing Systems," *2019 IEEE Wireless Communications and Networking Conference Workshop (WCNCW)*, Marrakech, Morocco, 2019, pp. 1-6.

[19] B. Han, S. Yuan, Z. Jiang, Y. Zhu and H. D. Schotten, "Robustness Analysis of Networked Control Systems with Aging Status," *IEEE INFOCOM 2020 - IEEE Conference on Computer Communications Workshops (INFOCOM WKSHPS)*, Toronto, ON, Canada, 2020, pp. 1360-1361.

[20] A. Arafa and S. Ulukus, "Age-Minimal Transmission in Energy Harvesting Two-Hop Networks," *GLOBECOM 2017 - 2017 IEEE Global Communications Conference*, Singapore, 2017, pp. 1-6.

[21] S. Leng and A. Yener, "Age of Information Minimization for an Energy Harvesting Cognitive Radio," *IEEE Transactions on Cognitive Communications and Networking*, vol. 5, no. 2, pp. 427-439, June 2019.

[22] O. M. Sleem, S. Leng and A. Yener, "Age of Information Minimization in Wireless Powered Stochastic Energy Harvesting Networks," *2020 54th Annual Conference on Information Sciences and Systems (CISS)*, Princeton, NJ, USA, 2020, pp. 1-6.

[23] M. Dabiri and M. J. Emadi, "Average Age of Information Minimization in an Energy Harvesting Wireless Sensor Node," *2018 9th International Symposium on Telecommunications (IST)*, Tehran, Iran, 2018, pp. 123-126.

[24] Y. Polyanskiy, H. V. Poor and S. Verdu, "Channel Coding Rate in the Finite Blocklength Regime," *IEEE Transactions on Information Theory*, vol. 56, no. 5, pp. 2307-2359, May 2010.

[25] B. Han, Z. Jiang, Y. Zhu and H. D. Schotten, "Recursive Optimization of Finite Blocklength Allocation to Mitigate Age-of-Information Outage," *2020 IEEE International Conference on Communications Workshops (ICC Workshops)*, Dublin, Ireland, 2020, pp. 1-6.

[26] S. Schiessl, J. Gross, M. Skoglund and G. Caire, "Delay Performance of the Multiuser MISO Downlink Under Imperfect CSI and Finite-Length Coding," in *IEEE Journal on Selected Areas in Communications*, vol. 37, no. 4, pp. 765-779, April 2019.

[27] J. Scarlett, V. Y. F. Tan and G. Durisi, "The Dispersion of Nearest-Neighbor Decoding for Additive Non-Gaussian Channels," in *IEEE Transactions on Information Theory*, vol. 63, no. 1, pp. 81-92, Jan. 2017.